

Localized Zero Modes and the Breakup of KAM Tori

Shau-Jin Chang and Alex Yurchenko

*Department of Physics, University of Illinois at Urbana-Champaign,
1110 West Green Street, Urbana, IL 61801-3080 U.S.A.*

(Received October 17, 1997)

The emergence of localized zero modes are responsible for the breakup of the KAM trajectories. These localized modes break the translational symmetry of the KAM trajectories, and transform these continuous KAM tori into cantori. A systematical method based on the above observation is used to calculate the zero modes and the critical parameter k_c .

PACS. 03.20.+i - Classical mechanics of discrete systems : general mathematical aspects.

I. Introduction

Kicked rotor model, in particular the Chirikov map, is a well-studied Hamiltonian system [1, 2]. It is known that as the strength k of the kick increases, more and more of the horizontal KAM trajectories disappear. As a KAM trajectory breaks up, the originally continuous torus develops an infinite number of gaps to become a cantorus [3]. The width of the largest gap scales as $(k - k_c)^\beta$ where k_c is the critical k at the breakup of the KAM trajectory. As we shall review in sec. 2, for $k < k_c$ there exists an extended zero mode corresponding to the translational symmetry of the KAM trajectory. This extended zero mode disappears for $k > k_c$. We conjecture that the breakup of a KAM trajectory is caused by the emergence of a localized zero mode in the associated lattice model. This particular nonlocal mode leads to instability for $k > k_c$, and causes the formation of tiny gaps in the form of a cantor set. In sec. 2 and 3, we review the variational principle and the translational zero mode. In sec. 4, we describe how a localized zero mode can cause the breakup of a KAM trajectory, and the forming of a cantorus. In secs. 5 and 6, we develop a method for obtaining the critical k_c and the zeromodes.

II. Variational principle

The kicked rotor system obeys the iterative equation,

$$p_{n+1} = p_n - V'(q_n), \quad (1)$$

$$q_{n+1} = q_n + p_{n+1} \pmod{1}, \quad (2)$$

where $V(q)$ is a periodic kick potential with period 1. The Chirikov map corresponds to the potential,

$$V(q) = \frac{k}{(2\pi)^2} \cos(2\pi q). \quad (3)$$

Eliminating p_n from (1) and (2), we obtain

$$q_{n+1} - 2q_n + q_{n-1} + V'(q_n) = 0 \pmod{1}. \quad (4)$$

If we drop the (mod 1) condition in Eq.(4), then q_n has the interpretation of the equilibrium position for a string of particles under the nearest neighbor potential $(q_{n+1} - q_n)^2/2$ and sitting on a periodic (lattice) potential $-V(q_n)$. The total energy of this lattice system is

$$W = \sum_n \frac{1}{2} (q_{n+1} - q_n)^2 - V(q_n), \quad (5)$$

where W also plays the role of an action in the kicked rotor model [3, 4]. It is easy to see that W is stationary under the variation of q_n . In the lattice model, q_n has the range from $-\infty$ to ∞ . The winding number ν in the kicked rotor model is related to the particle density of the lattice model by

$$\lim_{n \rightarrow \infty} \frac{n}{q_n - q_0} = \frac{1}{\nu}. \quad (6)$$

When the kick potential is weak, the horizontal KAM trajectory exists for most of the irrational winding number ν . As the strength of the potential increases, these KAM trajectories gradually disappear. We are interested in the mechanism of their disappearance.

When the KAM trajectory with winding number ν exists, we can parametrize p and q on this trajectory by a new variable θ ,

$$p = p(\theta), \quad q = q(\theta). \quad (7)$$

In (7), $p(\theta)$ is a periodic function of θ with period 1, and $q(\theta)$ increases by 1 as θ increases by 1,

$$q(\theta + 1) = q(\theta) + 1. \quad (8)$$

Along a KAM trajectory, we can introduce an averaged action per iteration in the kicked rotor system as [3, 4]

$$\begin{aligned} \mathcal{W} &= \lim_{N \rightarrow \infty} \frac{1}{N} \sum_{n=1}^N \left[\frac{1}{2} (q_{n+1} - q_n)^2 - V(q_n) \right] \\ &= \int_0^1 d\theta \left[\frac{1}{2} (q(\theta + \nu) - q(\theta))^2 - V(q(\theta)) \right]. \end{aligned} \quad (9)$$

As one varies $q(B)$, we obtain

$$q(\theta + \nu) - 2q(\theta) + q(\theta - \nu) + V'(q(\theta)) = 0, \quad (10)$$

which is the kicked rotor equation along a KAM trajectory.

III. Translational invariance and zero modes

The presence of a KAM trajectory implies that the averaged action per iteration, \mathcal{W} , is invariant under the translation of θ . In the associated lattice model, this implies that the averaged energy per particle over a large n is invariant under the translation of θ ,

$$\delta q_n = q'(\theta_n)\delta\theta, \quad (11)$$

where $\theta_n = \theta_0 + n\nu$. Just as a Goldstone mode in field theory, this translational symmetry leads to the existence of a zero mode. For simplicity, we consider the case that the energy is indeed the minimum for this particular winding number. The terms linear in δq vanish because their coefficients obey kicked rotor equation. We keep all the second order terms, obtaining

$$W = W_0 + \sum_n \left[\left(1 - \frac{1}{2} V''(q_n) \right) \delta q_n^2 - \delta q_{n+1} \delta q_n \right], \quad (12)$$

where W_0 is the energy evaluated at $\delta q_n = 0$. Eq. (12) can be written in the matrix form

$$W = W_0 + \mathbf{t} \frac{1}{2} \sum_{m,n} \delta q_m L_{mn} \delta q_n, \quad (13)$$

where the only nonvanishing matrix elements of \mathbf{L} are

$$\begin{aligned} L_{nn} &= 2 - V''(q_n), \\ L_{n,n+1} &= L_{n+1,n} = -1. \end{aligned} \quad (14)$$

Since \mathbf{W} is bounded from below by W_0 , all eigenvalues of \mathbf{L} are nonnegative. When the KAM trajectory exists, the translation mode described in Eq. (11) leaves \mathbf{W} unchanged and this set of variations (δq_n) gives rise to a zero mode of \mathbf{L} . Note that $q'(B)$ is a periodic function of θ and hence is also a periodic function of $q \pmod{1}$. This zero mode eigenfunction of \mathbf{L} forms an extended wave function in q space. As we increase the kick potential beyond certain strength, the horizontal KAM will breakup and cease to exist as a KAM trajectory. At this point, the translational symmetry of the solution on the KAM trajectory will cease to exist. The extended zero mode wave function which comes with it will also disappear.

The presence and absence of extended zero modes have a simple physical realization in the lattice model. When the KAM trajectory exists in the kicked rotor model, the string of particle in the associated lattice model can be pulled along continuously without changing the energy. During the pulling of a string of particles, the energy required at one part of the string is provided by the release of energy at another part. The string is not pinned at any particular position. When the KAM trajectory is broken up, the string is pinned at many (actually an infinite number of) places. It will make an infinite number of jumps as the string moves along.

IV. Localized zero modes and cantori

For definiteness, we introduce parameter k to describe the strength of the kick, as in the Chirikov map. For a given winding number ν , there is a critical strength k_c under which ($k < k_c$) the KAM trajectory exists, and above which ($k > k_c$) the KAM trajectory breaks up. We shall investigate the mechanism of this breaking up. For $k < k_c$, all eigenvalues of the matrix L are nonnegative. There is one zero mode eigenstate of matrix L which is extended in q space. Chang conjectured earlier that a localized zero mode eigenstate of L appears at the critical coupling k_c . We can understand qualitatively the effect of this zero mode by the mean field treatment as follow: For k slightly smaller than k_c , this localized eigenstate has a slightly positive eigenvalue and does not affect the stability of the KAM trajectory. We denote this localized eigenvector by v , and obtain the matrix equation

$$\sum_m L_{mn} v_n = a(k_c - k)v_m, \quad (15)$$

where a is a positive constant. We choose the normalization

$$\sum_n |v_n|^2 = 1. \quad (16)$$

The energy associated with such a variation,

$$\delta q_n = \delta \lambda v_n, \quad (17)$$

is

$$W = W_0 + a(k_c - k)(\delta \lambda)^2 + b(\delta \lambda)^3 + c(\delta \lambda)^4 + \text{high order terms}. \quad (18)$$

Since v_n is the first local zero mode, we have $b = 0$ and $c > 0$. Eq. (18) is the mean field equation of a second order phase transition. Parameter $\delta \lambda$ plays the role of an order parameter. In the mean field approximation and for $k < k_c$, the minimum of W given by Eq. (18) is at $\delta \lambda = 0$. On the other hand for small and positive $k - k_c$, the minimum of W occurs at

$$\delta \lambda = \pm \sqrt{\frac{a}{2c}}(k - k_c)^{1/2}, \quad (19)$$

and is

$$W = W_0 - \frac{a^2}{4c}(k - k_c)^2. \quad (20)$$

To the first approximation, one expects that the minima of W of (18) occur at $q_n \pm \delta \lambda v_n$. The region of q_n in between is now a region where W reaches a local maximum. The particle will avoid this region in its true minimum energy state. As a result, the places where the particles avoid will become gaps in the particle distribution. When we map a lattice solution into a kicked rotor solution, these gaps are mapped to tiny holes on the KAM trajectory and give rise to the observed cantorus. The width of the largest holes of the cantorus is given by the order parameter $\delta \lambda$.

V. Fibonacci cycles and distribution numbers

The appearance of localized zero modes may be used to calculate the critical parameter k_c . We start with the computation of new periodic orbits with winding numbers given by the ratios of Fibonacci numbers. For sufficiently small values of k , there are exactly two periodic orbits for each winding number. In terms of the lattice description, one of the orbits is the true minimum. However, as k increases, additional periodic orbits start to appear. We shall describe the condition of their appearance, and their relation to the zero mode.

Consider periodic orbits with winding number $5/8$. They denote period-8 orbits with a total advance of winding number 5. For small k , there are exactly two such orbits as noted earlier. For $k > 1.892347$, a new pair of period-8 orbits with the same winding number appear. As k increases, more cycles appear rapidly. To categorize these new cycles, it is convenient to introduce the concept of distribution numbers. In terms of lattice gas description, a periodic orbit is represented by a cyclic distribution of particles in a lattice of periodic potentials. A $5/8$ orbit represents putting 8 particles in 5 periodic potential wells. For the ground state, the particle distribution numbers in these 5 wells are 12212. The new orbits appeared at $k = 1.892347$ have the distribution numbers 21122. Because of the periodic nature of the orbits, cyclic permutations of these distribution represent the same orbit.

When we study orbits whose winding numbers are the ratios of two Fibonacci numbers, F_n/F_{n+1} , an inflation rule originally introduced in the construction of nonperiodic tilings and quasicrystals become extremely valuable [5]. For instance, we can obtain the corresponding distribution numbers for $8/13$ orbits from those of $5/8$ orbits by the replacement rules,

$$1 \rightarrow 2, \quad 2 \rightarrow 21.$$

These lead to the distribution numbers 22121221 for the original orbits, and 21222121 for the first pair of new orbits. We can use the inflation rule to obtain the required distribution numbers for orbits of any winding number F_n/F_{n+1} . It should be emphasized that these two sets of distribution numbers can be transformed into each other by switching one pair of 1 and 2 at two symmetric locations. For instance, the above $8/13$ orbits can be transformed into each other by switching $1 \leftrightarrow 2$ at locations 2 and 3, and/or at locations 5 and 6. As we shall see, these two locations are crucial in our understanding of zero modes.

Armed with the information on the distribution numbers, we can determine unambiguously the critical k values associated with the first appearance of the corresponding new orbits. These new orbits all appear through tangent bifurcations.

VI. Computation of the critical k

In the numerical calculation of the critical k for a given orbit, we first choose a higher k , and follow Greene's method [2] to seek out the orbit with desired distribution numbers. Once the orbit is found, we then lower the k until it reaches the critical value. For k larger than the critical value, there exist two orbits with the desired distribution numbers. For k smaller than the critical value: there are none. We are able to use the above property

to determine the critical k . In Table I, we list the critical values of k_n for all cycles up to $n = 17$ and $F_n/F_{n+1} = 4181/6765$.

As we can see, k_n approaches a limit at large n geometrically [6],

$$k_n \approx k_\infty + A/\delta^n. \quad (21)$$

Taking the above formula as exact, one can obtain k_∞ and δ from three sequential k_n ,

$$\delta = \frac{k_{n-1} - k_n}{k_n - k_{n+1}}, \quad \text{and} \quad k_\infty = \frac{k_{n+1}\delta - k_n}{\delta - 1}.$$

Based on the last 5 k_n , we obtain the following values of k_∞ and δ :

n	δ	k_∞
15	1.630	0.971637
16	1.630	0.971638
17	1.629	0.971636

which are consistent with the existing numbers [3]

$$k_\infty = 0.971635, \quad \delta = 1.6280$$

TABLE I. Critical k_n

n	F_n/F_{n+1}	k_n
4	5/8	1.8923469133
5	8/13	1.4577317529
6	13/21	1.2449326755
7	21/34	1.1318796973
8	34/55	1.0667374989
9	55/89	1.0291102636
10	89/144	1.0064820164
11	144/233	0.9929130639
12	233/377	0.9846412648
13	377/610	0.9796066770
14	610/987	0.9765228087
15	987/1597	0.9746350639
16	1597/2584	0.9734767121
17	2584/4181	0.9727661051
18	4181/6765	0.9723297764

VII. Zero modes

Our periodic orbit calculations provide us a way for obtaining the localized zero mode at k_c . As we have conjectured earlier, the appearance of this localized zero mode is responsible for the breakdown of the last KAM trajectory. In our study of new orbits with winding number F_n/F_{n+1} , these new orbits appear through tangent bifurcations. At a tangent bifurcation, the energy is stationary along the bifurcation direction and leads to a zero mode. This zero mode is localized around the sites where the distribution numbers are different from those of the original states. Here, we wish to make a quick clarification of our language. In the following lattice calculation, we keep the Bloch momentum to be zero. Under this condition, we have exactly N eigenstates for small variations around a period- N orbit. When we take the full range of Bloch momentum into account, each of the above discrete states will develop into a narrow band. Thus for the periodic orbit calculation, zero modes are really approximate zero eigenvalue band.

As we have mentioned in Sec. 4, there are exactly two sites where the distribution numbers are switched. Indeed, there are also two approximate zero eigenmodes (in the sense mentioned above) localized around these sites. Just like in a double well potential, the eigenvectors are the symmetric and the antisymmetric combinations of these localized states. One of the eigenstates is the zero eigenvalue associated with the tangent bifurcation. The other one has extremely small eigenvalue for a large Fibonacci F_n . As $n \rightarrow \infty$, these zero modes all converge to the unique localized zeromode at k_c .

In Fig. 1, we plot the two lowest eigenfunctions associated with the small variations around the new 55/89 orbit. Fig. 1(a) describes the ground state eigenfunction with eigenvalue -0.001017. Defined on a circle, this eigenfunction is symmetric with respect to the lattice positions 0 and 44/45. Fig. 1(b) describes the first excited eigenfunction with eigenvalue to be zero exactly, corresponding to the small variation along the tangent bifurcation direction. This eigenfunction is antisymmetric with respect to locations 0 and 44/45. Both eigenfunctions peaked at locations 17 and 72. These peaks sit precisely at the locations where the new orbit are different from the original orbit. As we consider a larger and larger F_n/F_{n+1} orbit, the corresponding zeromodes always have the same qualitative structure but with larger separation between the peaks. The difference of the two "zeromodes" eigenvalues vanishes exponentially with their separation. The difference measures the overlapping of the wave functions located at the different peaks. In Fig. 2, we present the localized zeromode constructed directly from the KAM trajectory at k_c . We can see the remarkable agreement of this zeromode with the 55/89 orbit zeromodes.

VIII. Discussions

At k slightly larger than k_c , one encounters an infinitely number of different possible orbits which makes the KAM curve in the Chirikov map unstable. It should be no surprising that there are many nearly degenerate localized eigenstates of L . We can visualize these states by the following picture. Let the winding number ν be approximated by a rational number M/N . Then, after N iterations along the KAM trajectory, we arrive at

$$q_{n+N} \approx q_n + M, \quad (22)$$

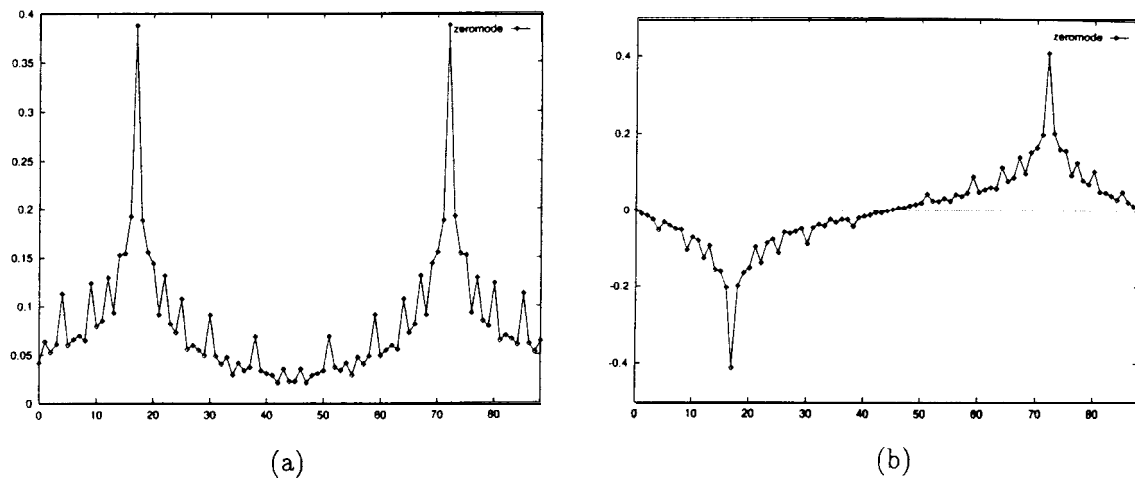


FIG. 1. Two lowest eigenfunctions associated with the small variations around the new $55/89$ orbit. These are an exact and an approximate zero eigenmode. The slight difference in eigenvalues is a measure of the overlap of the wave functions associated with the separate peaks, and the difference vanishes exponentially with the separation of the peaks. (a) Symmetric wave function with the lowest eigenvalue -0.001017 . (b) The antisymmetric wave function with zero eigenvalue.

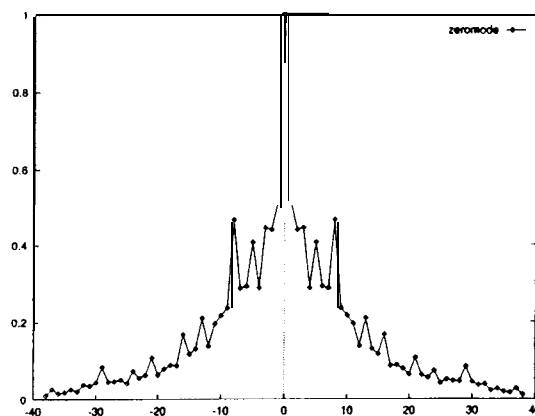


FIG. 2. The localized zeromode associated with the small variations around the last KAM trajectory at the critical parameter $k_c = 0.971635$.

and the lattice is nearly periodic. For most of the irrational number ν , the correction to the above equation is of $O(1/N^2)$ or smaller. Thus, at k_c , $u_n \equiv v_{n+N}$ is an approximate zero-mode eigenstate. From these nearly degenerate eigenstates, we can construct approximate zero-mode wave functions of all scales. The true minimum energy states of lattice model at k_c should involve eigenstates of \mathbf{L} of all different scales. One expects that renormalization group approach should play an important role in our understanding of this interesting problem [7, 8].

Acknowledgments

Alex Yurchenko was an REU student at the physics department of the University of Illinois during the summer of 1997. He was participating in an REU summer program supported by the US National Science Foundation under the grant number NSF PHY 93-22320. Eric Weeks worked on a similar research problem in the past, and Abdelhamid Galal works on a related problem. SJC wishes to thank them for their helps. SJC is also indebted to Robert MacKay for a stimulating conversation.

References

- [1] V. B. Chirikov, *Phys. Rep.* **52**, 263 (1979).
- [2] J. M. Greene, *J. Math. Phys.* **20**, 1183 (1979).
- [3] R. S. MacKay, J. D. Meiss, and I. C. Percival, *Physica* **13D**, 55 (1984).
- [4] I. C. Percival, *J. Phys.* **12A**, L57 (1979).
- [5] The phenomenon of inflation and deflation in nonperiodic tilings was discovered by Roger Penrose. An article on nonperiodic tilings by M. Gardner in *Scientific American*, Jan. 1977, pp. 110-121 is extremely readable. The concept and origin of the idea of inflation and deflation are discussed in this article. For a survey of papers on quasicrystals and their physical applications, see *The Physics of Quasycrystals*, eds. P. J. Steinhardt and Stellan Ostlund, (World Scientific, Singapore, 1987).
- [6] This is the typical behavior when the system is self-similar under an inflation rule. It suggests an underlying renormalization group construction. This is quite similar to the self-similarity behavior studied by M. Feigenbaum in *J. Stat. Phys.*, **19**, 25 (1978).
- [7] K. G. Wilson and J. Kogut, *Phys. Rep.* **12**, 75 (1974).
- [8] S. K. Ma, *Modern Theory of Critical Phenomena* (Benjamin, 1976).